AD-A157 751 DESIGN OF TRANSVERSELY STIFFENED FRP (FIBRE-REINFORCED PLASTIC) PANELS UN..(U) ADMIRALTY MARINE TECHNOLOGY ESTABLISHMENT DUNFERMLINE (SCOTLA.. C S SMITH DEC 84 1/1

UNCLASSIFIED AMTE(S)-R84104 DRIC-BR-94017 F/G 11/9 NL

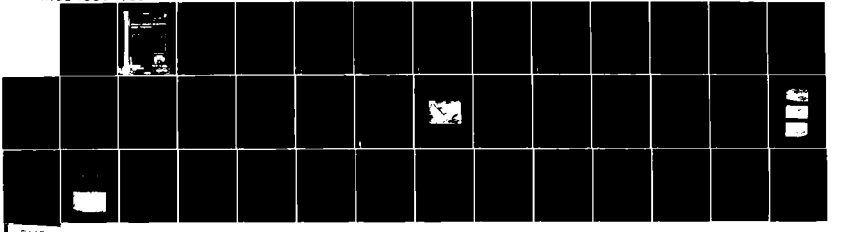

END
DATE FILMED
3-85

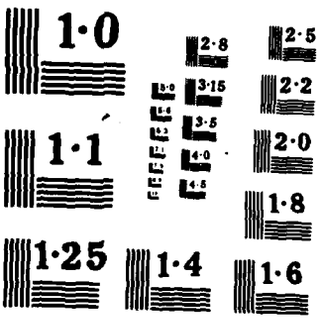
1·0
1·1
1·25
1·4
1·6
1·8
2·0
2·2
2·5
2·8
3·15
3·5
4·0
4·5

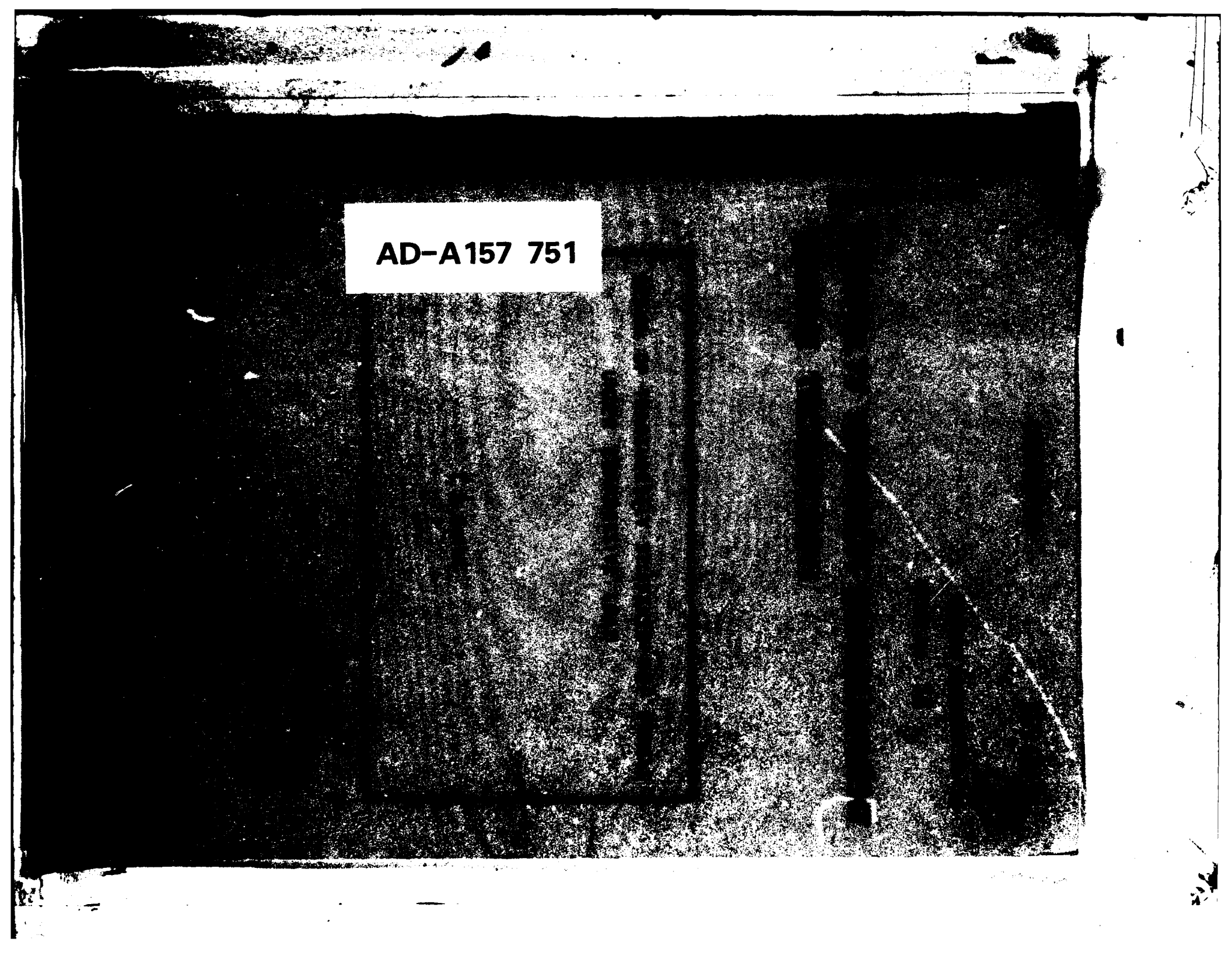
AD-A157 751

AMTE(S) R84104

DESIGN OF TRANSVERSELY STIFFENED FRP PANELS UNDER COMPRESSIVE LOAD (U)

BY

C S SMITH

Summary (U)

A review is made of the problem of buckling failure in fibre-reinforced plastic panels having stiffeners of "hat" section under compressive load acting across the line of the stiffeners. This problem is of practical importance in the design of FRP ships. Alternative analysis methods are discussed, including use of approximate data curves and folded-plate analysis to determine initial buckling behaviour, together with nonlinear finite element analysis referring to imperfection effects and post-buckling behaviour. Some previously unreported experimental results are described. These, together with previously published test data, are correlated with theoretical analysis as a basis for making up-dated design recommendations.

ARE Dunfermline
St Leonard's Hill
DUNFERMLINE Fife KY11 5PW

December 1984

CONTENTS

DESIGN OF TRANSVERSELY STIFFENED FRP PANELS UNDER COMPRESSIVE LOAD (U)

INTRODUCTION

Fibre-reinforced plastics are now used very extensively in the boatbuilding industry, accounting for construction of about 80% of small boats up to 25 m in length including pleasure craft, workboats and fishing boats. FRP construction, based usually on the use of polyester resin reinforced by E-glass fibres in the form of chopped-strand mat or woven-rovings together with a limited amount of unidirectional tape in stiffeners, is also widely employed in larger ships including military patrol craft up to 40 m in length and minesweepers of up to 60 m (1)*.

2. The need for general robustness and high strength under transverse load leads in many cases to adoption of transversely framed hulls, as illustrated in Figure 1, containing few, if any, longitudinal stiffeners. Shell and deck panels designed in this way are clearly less efficient than longitudinally stiffened panels in resisting longitudinal compression associated with hull bending: except in weight-critical hulls such as fast patrol craft, however, the weight penalty associated with transverse framing appears to be preferable to the additional complexity and hence cost of fabricating a system of orthogonal stiffening. Hull designers are therefore frequently faced with the need to evaluate the compressive strength of transversely stiffened deck and shell panels, as illustrated in Figure 2.

3. For structural design purposes a ship's hull can usually be treated as an assembly of stiffened panels which may be examined individually assuming either simple support or appropriate conditions of elastic support at the boundaries. Unlike longitudinally framed panels, whose elastic stability is inherently greater and in which a substantial post-buckling reserve of strength may exist, transversely stiffened structures are likely to fail catastrophically at loads approximately equal to theoretical critical values and must therefore be designed with extreme care against elastic buckling. Glass-reinforced plastic (GRP) panels are particularly susceptible to instability because of their low material stiffness (Young's modulus/compressive strength typically < 80). Buckling behaviour is complicated by the anisotropic nature of the material and the "hat" form of stiffeners normally used in GRP hull construction.

4. A theoretical study carried out previously (2) has identified various forms of instability occurring in transversely stiffened FRP panels and has established approximate data curves and accurate computer-based analysis methods for evaluation of initial buckling stresses and mode shapes. Compression tests on small-scale perspex and GRP models (3,4,5) and a limited number of large-scale GRP panels (6) have provided some confirmation of theoretical predictions. The purpose of the present report is to assemble all available experimental data, including some previously unreported results of tests on large-scale GRP panels, to extend theoretical analysis by consideration of nonlinear buckling behaviour and imperfection sensitivity, to correlate test data with alternative theoretical estimates of buckling strength and hence to draw up recommendations for improved design of transversely stiffened GRP panels under compressive load.

---

*( ) = References on page 16

ANALYSIS METHODS

5. Assuming simple support at the longitudinal edges (y = 0, B), initial buckling loads N_{xcr} and corresponding mode shapes for a longitudinally compressed, transversely stiffened GRP panel may be evaluated using the methods outlined below.

Folded-Plate Analysis

6. A stiffened panel as shown in Figure 2 is treated as an assembly of rectangular plate strips corresponding to frame webs and tables and to elements of shell laminate contained within and lying between hat-section stiffeners. Each plate strip is related to x and y axes parallel to its width b and length B respectively and is assumed to have principal directions of elasticity parallel to its sides and hence to satisfy the orthotropic plane stress-strain relationship

$$\begin{bmatrix} \epsilon_x \\ \epsilon_y \\ \gamma_{xy} \end{bmatrix} = \begin{bmatrix} \frac{1}{E_x} & \frac{-\mu_x}{E_y} & 0 \\ \frac{-\mu_y}{E_x} & \frac{1}{E_y} & 0 \\ 0 & 0 & \frac{1}{G_{xy}} \end{bmatrix} \begin{bmatrix} \sigma_x \\ \sigma_y \\ \tau_{xy} \end{bmatrix} \quad \ldots\ldots\ldots\ldots \quad (1)$$

Reinforcing fibres are assumed to be stacked symmetrically about the mid-thickness of the laminate so that no direct coupling occurs between membrane and bending deformations: the moment-curvature relationship for the strip is then

$$\begin{bmatrix} m_x \\ m_y \\ m_{xy} \end{bmatrix} = -\begin{bmatrix} D_x & \mu_x D_x & 0 \\ \mu_y D_y & D_y & 0 \\ 0 & 0 & D_{xy} \end{bmatrix} \begin{bmatrix} \frac{\partial^2 w}{\partial x^2} \\ \frac{\partial^2 w}{\partial y^2} \\ 2\frac{\partial^2 w}{\partial x \partial y} \end{bmatrix} \quad \ldots\ldots\ldots\ldots \quad (2)$$

where $D_x = E_x h^3/\left[12\ (1 - \mu_x\mu_y)\right]$ and $D_y = E_y h^3/\left[12\ (1 - \mu_x\mu_y)\right]$ are flexural

rigidities per unit width in x and y-directions and $D_{xy} = G_{xy}h^3/12$ is the twisting rigidity. These conditions of elasticity are effectively satisfied by most marine-type GRP laminates based on chopped strand, woven-roving and unidirectional reinforcement.

7. Equilibrium and compatibility considerations lead to the following pair of equations in the in-plane displacements u and v of a plate strip subjected to a uniform destabilizing force per unit width N_x in the x-direction.

$$\frac{E_x}{1 - \mu_x\mu_y}\left[\frac{\partial^2 u}{\partial x^2} + \mu_x \frac{\partial^2 v}{\partial x \partial y}\right] + G_{xy}\left[\frac{\partial^2 v}{\partial x \partial y} + \frac{\partial^2 u}{\partial y^2}\right] = 0 \quad \ldots\ldots\ldots \quad (3)$$

$$\frac{h E_y}{1 - \mu_x\mu_y}\left[\frac{\partial^2 v}{\partial y^2} + \mu_y \frac{\partial^2 u}{\partial x \partial y}\right] + h G_{xy}\left[\frac{\partial^2 v}{\partial x^2} + \frac{\partial^2 u}{\partial x \partial y}\right] - N_x \frac{\partial^2 v}{\partial x^2} = 0 \ldots \quad (4)$$

Similarly the equation governing bending displacements w is found to be

$$D_x \frac{\partial^4 w}{\partial x^4} + 2H \frac{\partial^4 w}{\partial x^2 \partial y^2} + D_y \frac{\partial^4 w}{\partial y^4} + N_x \frac{\partial^2 w}{\partial x^2} = 0 \quad \ldots\ldots\ldots \quad (5)$$

where $H = 2 D_{xy} + \mu_x D_x$

The conditions of simple support at y = 0, B (ie $u = \partial v/\partial y = 0$ and $w = \partial^2 w/\partial y^2 = 0$ at y = 0, B) allow solutions of equations 3, 4 and 5 to be assumed of the form

$$\left.\begin{aligned} u &= u_1 \sin \alpha y \\ v &= v_1 \cos \alpha y \\ w &= w_1 \sin \alpha y \end{aligned}\right\} \quad \ldots\ldots\ldots \quad (6)$$

in which $\alpha = \pi/B$ and u_1, v_1 and w_1 are functions of x independent of y. Substitution of (6) in equations 3, 4 and 5 leads to a set of ordinary differential equations in u_1, v_1 and w_1 whose solutions, depending on the boundary conditions at x = 0, b, are readily found. By adopting as boundary conditions unit displacements u_1, v_1, w_1 and rotations dw_1/dx at the edges x = 0, b and by substitution of the resulting expressions for u, v and w in equations 1 and 2, a matrix of stiffness coefficients may be established for each plate element. Combination of element stiffness coefficients under conditions of continuity between plate strips yields a set of 4n homogeneous equations which express the equilibrium of sinusoidally distributed moments and forces at all n plate intersections or node lines in the idealized structure. These equations correspond to a standard eigenvalue problem which may be written in matrix form

$$K \delta_1 = 0 \qquad \ldots\ldots\ldots\ldots \quad (7)$$

where K is a square stiffness matrix and δ_1 is a column matrix defining a buckling mode. In general an infinite number of eigenvalues and eigenvectors exist, each satisfying equation 7 and corresponding to a particular buckling mode. Buckling loads may be found by varying systematically the value of N_x and evaluating the determinants of corresponding stiffness matrices K: critical values N_{xcr} are those for which the determinant of K is zero. This process can be carried out automatically on a computer with buckling loads calculated by iteration to any required accuracy. When a critical value of N_x has been found the corresponding normalized mode may be obtained by setting one of the nodal displacements or rotations equal to unity and reducing the homogeneous equations (7) to a set of one fewer nonhomogeneous equations which are solved in the usual way by matrix division. Intermediate modal displacements and stresses may finally be computed at any point on each plate to obtain a complete definition of the buckling mode.

8. The analysis method outlined was developed from a previous generalized treatment of folded plates under distributed and concentrated lateral loads (7). Buckling under compressive load N_y applied in the direction of stiffeners or biaxial compression may be examined by adding appropriate terms to equations 3, 4 and 5 and natural frequencies and modes of vibration may also be evaluated by including inertia terms in the plate equations (8). Analysis of this type has been developed independently by Wittrick and Williams (9,10), allowing additionally for the destabilizing effect of shear stresses in plate elements and for somewhat more general conditions of material anisotropy, and has been applied more recently by Viswanathan et al (11).

9. Application of folded-plate analysis to the idealized problem shown in Figure 2 has established that the lowest initial buckling stress usually corresponds to a local, interframe mode having one of the forms shown in Figure 3(a) (2). Exceptionally, in structures with a large width B, these modes may be preceded by Type-4 instability having either (or any linear combination) of the forms shown in Figure 3(b). Folded-plate analysis provides an economical and theoretically exact method of examining such instability. In a structure of "infinite" length analysis may be confined to a single frame-space, or half frame-space, bounded by planes of symmetry and/or antisymmetry depending on the mode shape under consideration; analysis may also be applied to a structure of finite length L as shown in Figure 2, with use of substructuring to achieve economy of computation for panels containing many identical frames.

Data Curves for Approximate Evaluation of Interframe Buckling

10. Guided by the exact buckling displacements and associated modal stresses computed using folded-plate analysis approximate models of interframe buckling have been established from which data curves may be derived as shown in Figure 4 and outlined below.

11. Type-1 buckling involves bending of the shell laminate restrained by flexural stiffness of the frame webs and tables with virtually zero displacement at intersections between the shell and frames. Provided that the transverse span B is large relative to the frame spacing $(b_1 + b_2)$, bending in the y-direction may be ignored and the shell treated as a continuous beam rotationally restrained at points of attachment to the frame. The buckling load per

unit width N_{xcr} is then independent of B, depending only on the flexural rigidity D_{x1} of the shell in the x-direction, the dimensions b_1 and b_2 and the restraining stiffness k_{F1} of the frame, given by

$$k_{F1} = a(1 - \frac{a}{4c})$$

where $a = 4D_{x4}/b_4$ and $c = a + 2D_{x3}/b_3$. Values of N_{xcr}, obtained by solution of a simple eigenvalue equation referring to rotation at the intersection of the shell and frame web, have been computed for a range of k_{F1} and b_1/b_2 and are plotted non-dimensionally in Figure 4(a) from which Type-1 buckling loads may be found for any practical frame-shell configuration. Assuming $b_1 > b_2$ it is evident that N_{xcr} is always greater than $\pi^2 D_{x1}/b_1^2$.

12. Type-2 interframe buckling involves bending of the shell restrained by torsional stiffness of the frame, with a modal half-wavelength equal to the frame spacing and a line of zero displacement at the centre of each frame. Buckling loads again depend on D_{x1}, b_1 and b_2 together with a coefficient k_{F2}, representing torsional stiffness of the frame, which is defined by

$$k_{F2} = \frac{2\pi^2 GJ}{b_2^2 B^2}$$

The effective torsional rigidity GJ is given by

$$GJ = 4A_o^2/\oint \frac{ds}{Gt} = 4A_o^2 \Big/ \left[\frac{b_2}{G_{xy}h_2} + \frac{b_3}{G_{xy}h_3} + \frac{2b_4}{G_{xy}h_4}\right]$$

where A_o is the area enclosed by the centrelines of the frame table and webs together with the enclosed portion of shell. Evaluation of buckling loads reduces to solution of an eigenvalue problem with two degrees of freedom referring to displacements and rotations at frame/shell intersections: values of N_{xcr}, which have been computed for a range of k_{F2} and b_1/b_2, may be found directly from Figure 4(b).

13. Type-3 interframe buckling, which involves bending of the shell with a modal half-wavelength equal to the frame spacing and lines of zero displacement mid-way between frames, is restrained by bending stiffness of the frames combined with a membrane shearing action in the shell between frames. This form of instability is less obviously predictable than Types 1 and 2 and is not a form of buckling likely to be encountered in panels with stiffeners of conventional, open cross-section. The fact that the preferred mode may involve flexural rather than torsional deformation of the frames is attributable to the high torsional rigidity of closed-section frames. Buckling loads are found to depend on D_{x1}, b_1, b_2 and a stiffness parameter k_{F3} which represents approximately the restraining influence of the frame and is given by

$$k_{F3} = \frac{\alpha^2}{2}\left[\alpha^2 EI + \frac{4h_1 e^2 \gamma_1}{b_1}\left(1 - \frac{4h_1\gamma_1}{\alpha^2 EAb_1 - 4h_1\gamma_1}\right)\right]$$

where h_1 is the shell thickness, EA and EI are axial and flexural rigidities of a composite section formed by the frame and enclosed portion of shell, e is the distance from the mid-plane of the shell to the centroid of that section, $\alpha = \pi/B$ and $\gamma_1 = G + \frac{\alpha^2 E_{y1} b_1^2}{12}$. Evaluation of buckling loads again reduces to solution of a two-degree-of-freedom eigenvalue problem: values of N_{xcr} for any k_{F3} and b_1/b_2 may be found from Figure 4(c).

14. Sufficient information is given above for use of the data curves shown in Figure 4: a more complete derivation of the curves may be found in Reference 2. Comparison with exact folded-plate solutions for a range of geometries has shown (2) that these curves give buckling stresses which differ usually by less than 10% from correct values, although errors may exceptionally be as much as 20%. Type-2 and Type-3 buckling modes, unlike Type-1, are sensitive to the width B of the panel. It is evident from Figure 4 and should be noted particularly that Type-2 and Type-3 buckling loads N_{xcr} may be less than the value $\pi^2 D_{x1}/b_1^2$: the assumption that interframe buckling corresponds to that of a simply supported strip of shell of width b_1, which has previously been made in design of transversely stiffened panels, is inadequate and unsafe.

Finite Element Analysis

15. Finite element analysis, employing shell elements in which anisotropic material properties and linear destabilizing (geometric stiffness) effects are represented, offers an alternative means of evaluating initial buckling stresses. Solutions obtained in this way for the idealized problem of Figure 2, although less accurate and more expensive in computing time, have been found to correspond quite closely with folded-plate solutions. The real merit of finite element analysis lies in its ability to deal with irregular structural geometry and boundary conditions: buckling solutions extending round the curved portion of structure at a ship's turn of bilge as shown in Figures 1 and 5 have for example been obtained in order to check boundary conditions assumed in the simpler models assumed for design purposes. As described below, finite element analysis may also be applied incrementally to examine the nonlinear buckling and post-buckling behaviour and imperfection sensitivity of stiffened panels.

EXPERIMENTAL RESULTS

Previous Test Results

16. In order to check the accuracy of analysis methods and in particular to verify theoretical predictions of Type-3 instability, compression tests were carried out on two small-scale flat rectangular panels (Models P1 and P2) with transverse hat-section frames, constructed in Perspex (polymethylmethacrylate), as illustrated in Figure 5(a). In order to check design assumptions relating to boundary conditions at a ship's centreline and turn of bilge, further tests were carried out on small-scale Perspex models of a vee-bottom structure incorporating a stiff keel girder (Model P3 as shown in Figure 5(b)) and a full hull

compartment (Model P4, Figure 5(c)). Model dimensions (defined as shown in Figure 6) and test results are summarized in Tables 1 and 3. In Model P3 the effective panel width B was taken as the distance from the centreplane to each edge while in Model P4 B was taken as the distance from the centreplane to the inside edge of the curved bilge. Mean measured properties of the Perspex material were found to be E = 2850 N/mm^2, μ = 0.37, UTS = 66 N/mm^2. A full description of these tests is given in Reference 3.

17. Small-scale experiments were followed by compression tests on three large-scale GRP structures (Panels 1, 2 and 3), results of which are outlined in Reference 6. Tests on two further large-scale GRP models (Panels 4 and 5), whose results have not previously been published, are described below. Tests have also been carried out on three GRP panels (S2, S3 and S4) representing at about 1/4-scale Panels 2, 3 and 4 (4,5). Dimensions, material properties and collapse strengths of test specimens are summarized in Tables 1, 2 and 3.

Panels 4 and 5

18. Test Panels 4 and 5, which corresponded to the bottom shell structure in a trial ship design, were nominally identical with an overall length of 609[illegible] mm and effective transverse span of 3048 mm. Each panel was stiffened by eight equally spaced transverse frames of hat-section. Fabrication was carried out, following standard shipyard procedures, using E-glass reinforcement and a ship-type isophthalic polyester resin. The shell laminate was reinforced by [illegible] plies of 800 g/m^2 woven rovings while the frames incorporated 14 plies of 800 g/m^2 WR with 12 plies of 600 g/m^2 unidirectional glass in the tables.

19. Tests were carried out in the large test frame at ARE in a rig developed for compression testing of large steel grillages (12). As shown in Figure [illegible], panels were supported horizontally on a steel platform and were held down at their ends by light flexure plates and along their sides by tie-bars with 150 mm spacing. This form of attachment was designed to impose conditions of simple support at the ends and sides of test panels, with ends and sides free to move longitudinally in-plane and sides also free to move transversely in-plane. The ends of transverse frames were restrained against torsional rotation. Longitudinal compression was provided by seven 1500 kN hydraulic jacks, evenly spaced across the ends of test panels, acting through calibrated hydraulic load transducers. Compression was applied by activating the jacks at one end of the structure from a common pressure source and reacting loads through a passive set of jacks at the other end. In order to distribute jack forces into test panels in a uniform manner, avoiding the risk of premature failure close to the ends, panels were reinforced by increasing the laminate thickness and fitting steel sandwich plates, bolted and bonded to the GRP, in the end bays. The sides of test panels were also reinforced by fitting short, discontinuous steel sandwich plates between transverse frames. The ends of hat-section frames were strengthened by short, built-in steel formers through-bolted to external steel pads.

20. Panel 5 was tested to collapse under compressive load alone while Panel 4 was tested under a combination of compressive load and uniform hydrostatic pressure. Lateral pressure was applied by means of a water-filled rubber bag contained between test panel and support platform as shown in Figure 7.

21. Before commencement of testing, initial deformations of each panel were surveyed: maximum interframe displacements w_o of the shell laminate, measured on a gaugelength equal to the frame spacing, together with maximum overall

displacements relative to the ends of the panels measured on the longitudinal centreplane, are listed in Table 1. Local distortions, significant in relation to interframe buckling, were generally very small (< B/3800) and were barely distinguishable from surface irregularities and variations in laminate thickness. The cov (standard deviation/mean value) of laminate thickness t_1 was 0.018 for Panel 4 and 0.009 for Panel 5. During tests, displacements were recorded at closely spaced positions along the centreplane of each panel. Strains were measured on both sides of the shell laminate and on frame tables as a basis for vertical alignment of jacks and as a check on the uniformity of compressive load.

22. Panel 5 was subjected to compressive load, applied incrementally with frequent removal of load to allow inspection for damage and to provide a check on permanent set and loss of stiffness. No significant damage, permanent distortion or loss of stiffness was observed up to an average compressive stress of 60 N/mm^2. At this stage crackling noises commenced and as load was increased whitening of the shell laminate was observed at the base of frame webs. Large buckling deformations developed as shown in Figure 9 and collapse finally occurred explosively at an average stress of 67.0 N/mm^2 taking the form of a fracture over the full width of the panel in the central bay. Failure of the shell laminate involved delamination with shear crimping and local buckling of the delaminated plies. A photograph of the collapsed panel is shown in Figure 8.

23. Panel 4 was subjected first to a uniform lateral pressure of 103 kN/m^2, causing overall bending deformation with an amplitude of 12.5 mm together with local interframe deformation of the shell laminate of maximum amplitude 0.5 mm. Lateral load was held constant at this level while compressive load was applied incrementally, simulating a design condition of combined compression and hydrostatic pressure. No damage was observed at compressive stresses of up to 60 N/mm^2. Collapse finally occurred across the full width of the central bay at an average stress of 65.8 N/mm^2. Progressive development of buckling deformations, superimposed on displacement caused by lateral pressure, is shown in Figure 10. Failure was very similar to that of Panel 5 and lateral pressure evidently had negligible influence on compressive strength.

CORRELATION WITH THEORETICAL BUCKLING ANALYSIS

24. A comparison of experimental collapse stresses with theoretical initial buckling stresses for Panels 4 and 5 and for the other GRP and perspex panels is made in Table 3. Theoretical buckling stresses were estimated in three different ways:

(i) from the data curves of Figure 4;

(ii) by application of folded-plate analysis to a single interframe span;

(iii) by application of folded-plate analysis to the full panel length.

It is evident that the data curves provide a reasonable first approximation to collapse strength, maximum positive and negative errors being +17% and -26% of experimental values. Folded-plate analysis provides a more accurate estimate of buckling strength with maximum errors of +5% and -20%. In the latter case (Panel P3) the conservatism of the theoretical estimate is attributable partly to the presence of a torsionally stiff longitudinal girder at one edge of the panel as shown in Figure 5(b): Panels 1, 3 and S3 were similarly affected by

the presence of a longitudinal edge-girder. Folded-plate analysis referring to interframe buckling evidently provides a close, slightly conservative approximation to the lowest initial buckling stress for a complete panel of finite length: analysis of a single interframe span should therefore normally be satisfactory for design purposes.

25. It may be noted that folded-plate calculations included the contribution of frame flanges, which effectively increase the shell thickness over a span b_F as shown in Figure 6. This effect was omitted (conservatively) from the data curves of Figure 4. Folded-plate solutions for Panel 5 neglecting frame flanges gave Type-1, Type-2, Type-3 and Type-4 buckling stresses which were respectively 2%, 1%, 8% and 6% less than values including flange effects.

26. Correlation of theoretical and experimental results is further summarized in the form of scatter diagrams, shown in Figure 11(a) and 11(b), referring to buckling stresses obtained respectively from data curves (Figure 4) and from interframe folded-plate analysis.

Modal Analysis of Experimental Buckling Deformations

27. As a means of improving the correlation of theoretical and experimental buckling behaviour which, as illustrated in Figure 9, may be complicated by occurrence of several closely spaced theoretical buckling stresses, experimental deformations were resolved into modal components using the orthogonal properties of theoretical modes. It was assumed that the k^{th} experimental displacement profile $\bar{w}_k$ for Panel 5, measured along the centreplane as shown in Figure 9, could be represented by

$$\bar{w}_k = \sum_{j=1}^{\infty} a_{jk} w_j \qquad \ldots\ldots\ldots (8)$$

where a_{jk} was an amplitude coefficient referring to the j^{th} normalized theoretical mode w_j. The orthogonality condition was assumed to be

$$\int_0^L w_i w_j \, dx = 0 \quad (i \neq j) \qquad \ldots\ldots\ldots (9)$$

taking x as the distance from one end of the panel. Coefficients a_{jk} were then found from the expression

$$a_{jk} = \int_0^L w_j \bar{w}_k \, dx \Big/ \int_0^L w_j^2 \, dx \qquad \ldots\ldots\ldots (10)$$

integrations being performed numerically using a general 3-ordinate Simpson's Rule. Deflection profiles do not in fact fully characterize buckling modes, which involve distortion of the frames and in-plane as well as bending deformation of the shell: the assumed orthogonality condition is therefore an approximation. It was however found from a numerical check on orthogonality

SMALL - SCALE PERSPEX MODELS

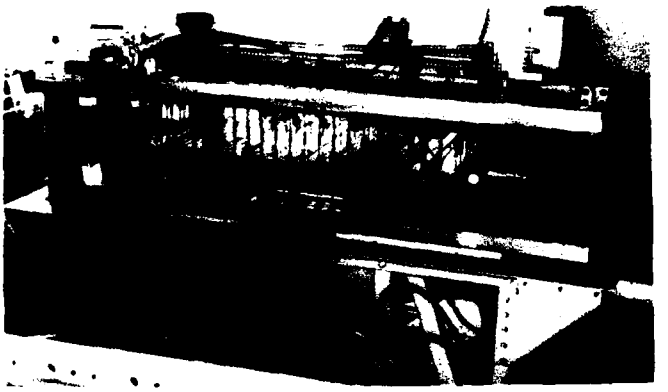

a) MODEL P1

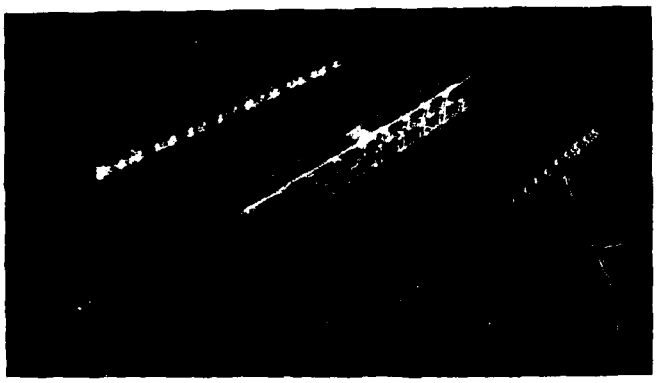

b) MODEL P3 - VEE BOTTOM STRUCTURE

c) MODEL P4 - HULL SECTION

FIGURE 5

DATA CURVES FOR TYPE - 3 INTERFRAME BUCKLING

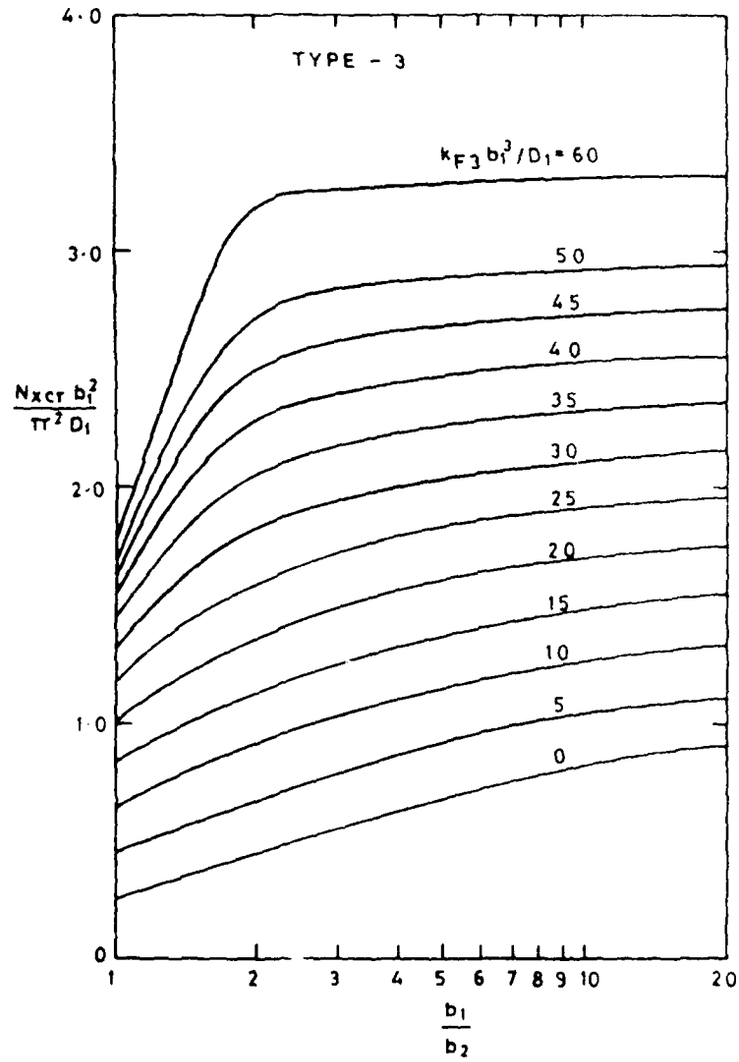

FIGURE 4c

DATA CURVES FOR TYPE - 2 INTERFRAME BUCKLING

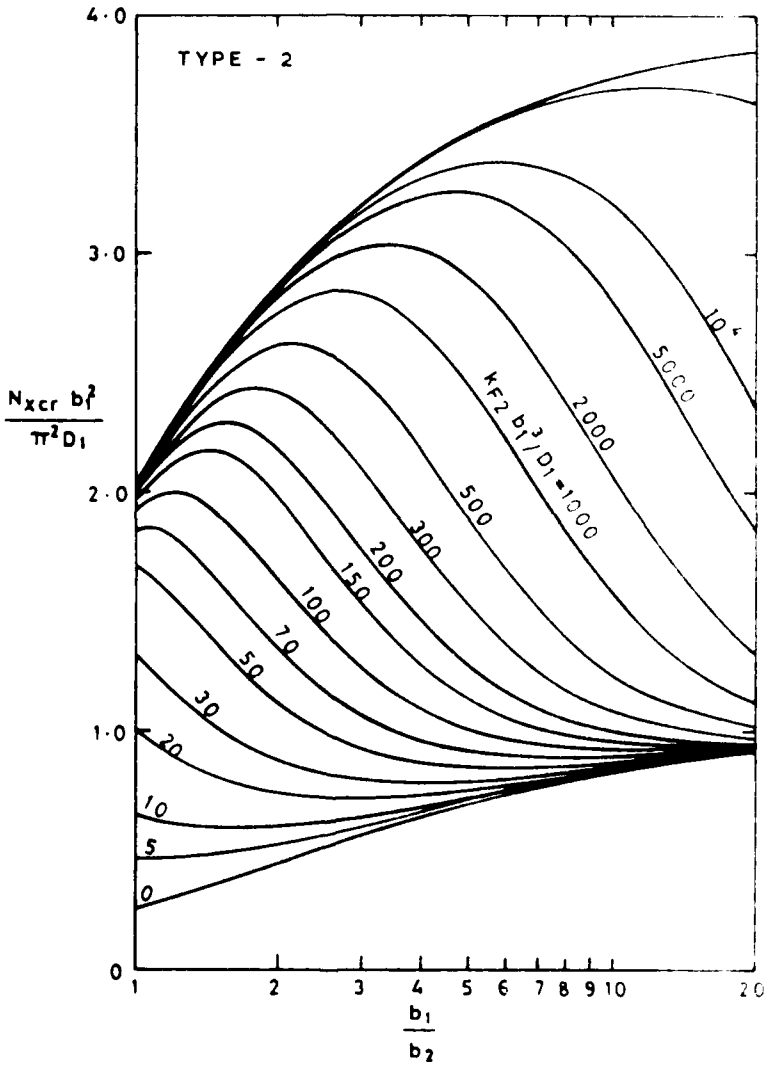

FIGURE 4b

DATA CURVES FOR TYPE-1 INTERFRAME BUCKLING

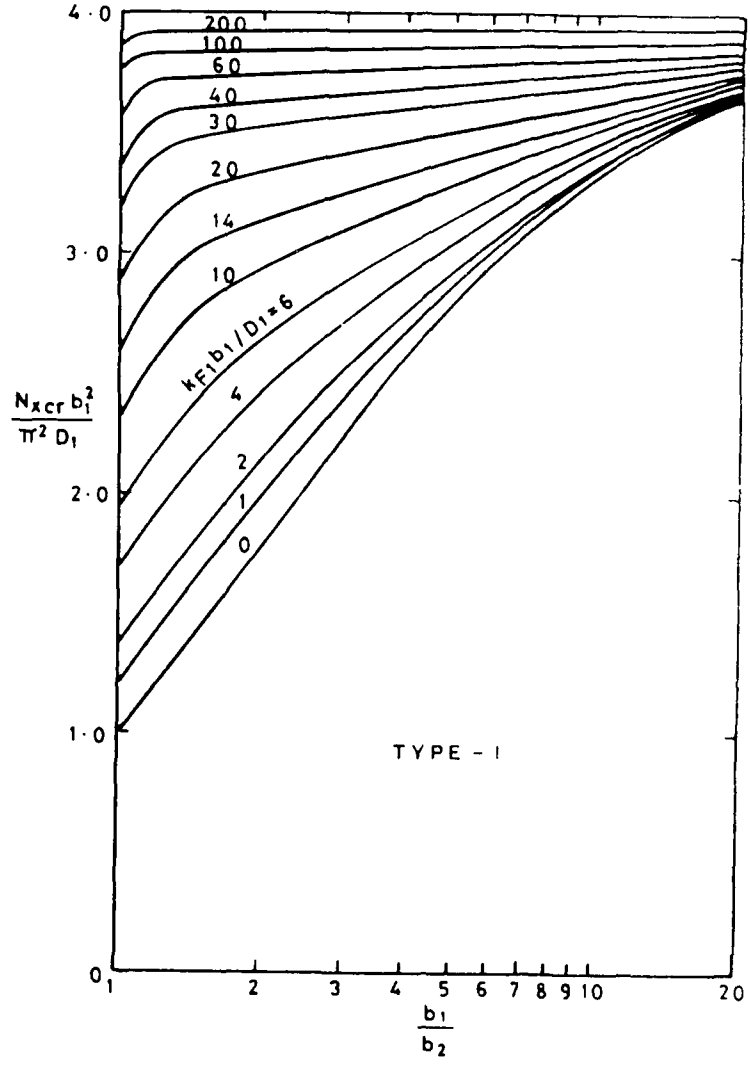

FIGURE 4a

LOCAL BUCKLING MODES

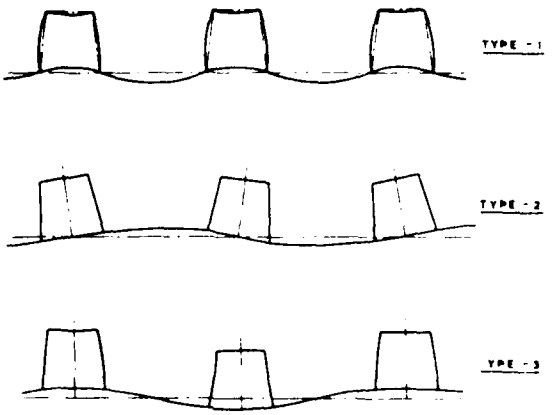

(a) INTERFRAME BUCKLING MODES

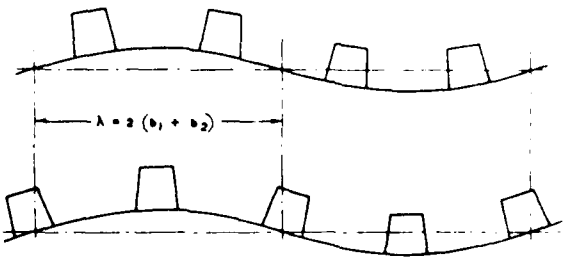

(b) TYPE - 4 BUCKLING

SL 72/116/1

FIGURE 3

IDEALIZED BUCKLING PROBLEM

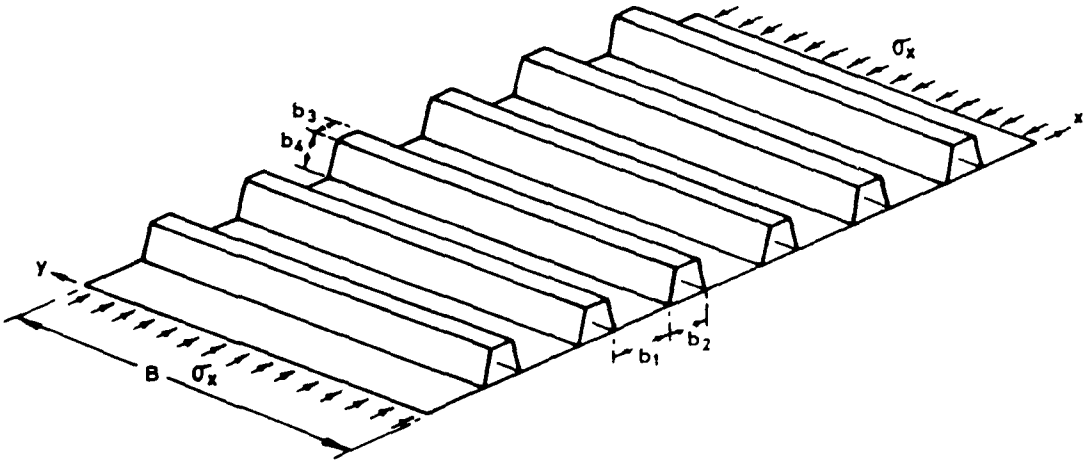

FIGURE 2

TEST SECTION SHOWING TRANSVERSELY FRAMED GRP HULL STRUCTURE

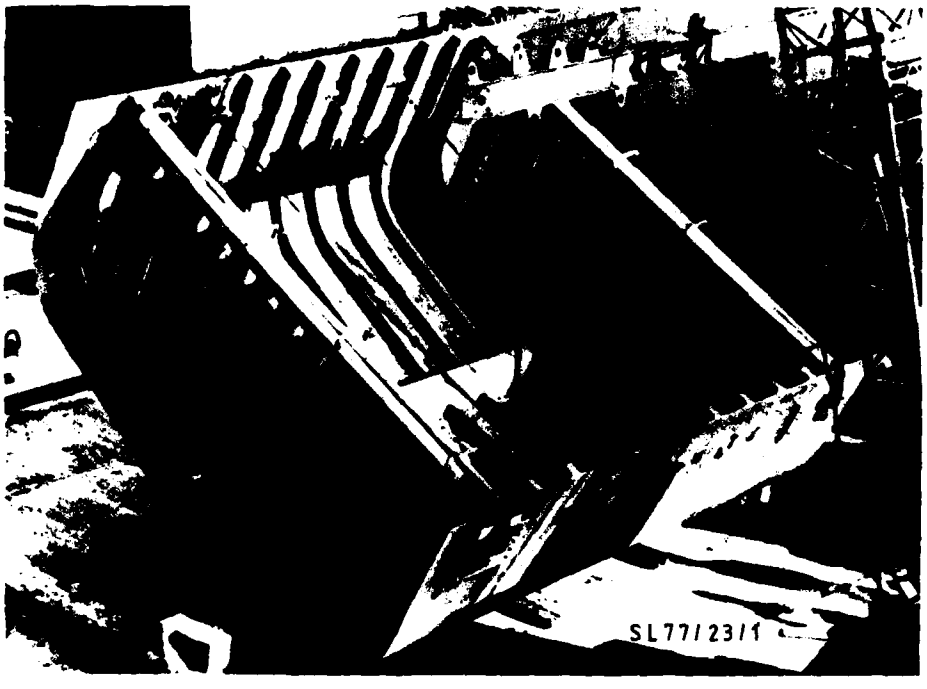

FIGURE 1

TABLE 3

CORRELATION OF EXPERIMENTAL COLLAPSE WITH THEORETICAL INITIAL BUCKLING BEHAVIOUR

	Experimental Failure		Theoretical Buckling Loads and Modes					
			Data Curves (Fig 4)		Folded-Plate Analysis			
					Interframe Buckling		Buckling over Full Panel Length	
	Collapse Stress (N/mm^2)	Buckling Mode	Buckling Stress (N/mm^2)	Mode	Stress (N/mm^2)	Mode	Stress (N/mm^2)	Mode
1	43.9	Predominantly Type 1	41.8	Type 3	37.3	Type 3	38.5	Type 3
			45.5	Type 1	47.6	Type 1	47.4	Type 1
2	56.9	Evidence of Type 2 and Type 1	54.6	Type 1	58.4	Type 1	58.7	Type 1
			67.2	Type 2	60.8	Type 4	59.7	Predominantly Type 1
3	80.0	Some Evidence of Type 2	93.8	Type 3	84.4	Type 3	86.7	Type 3
			110.0	Type 2	103.0	Type 2	100.0	Evidence of Type 2/Type 3
4	65.8	see Fig 11	67.7	Type 3	65.6	Type 3	67.0	Type 3
			84.9	Type 2	87.4	Type 4	72.8	see Fig 9
5	67.0	see Fig 9	67.7	Type 3	65.6	Type 3	67.0	Type 3
			84.9	Type 2	87.4	Type 4	72.8	see Fig 9
S2	63.4	Evidence of Type 2 and Type 3	54.8	Type 1	58.3	Type 1	66.2	Predominantly Type 1
			65.7	Type 2	67.4	Type 3	75.4	Predominantly Type 2
S3	79.3	Some evidence of Type 1	80.0	Type 1	77.5	Type 3	79.9	Predominantly Type 3
			89.7	Type 3	87.7	Type 1	86.7	Predominantly Type 1
S4	73.8	Evidence of Type 3 and Type 4	65.7	Type 3	65.4	Type 3	-	-
			92.8	Type 2	93.3	Type 4		
P1	10.9	Type 3/Type 4	10.0	Type 3	11.0	Type 3	11.1	Type 3
			17.7	Type 2	14.7	Type 4	11.5	Type 3/Type 4
P2	15.6	Well-defined Type 3	13.1	Type 3	13.5	Type 3	13.7	Type 3
			19.6	Type 2	15.1	Type 2	14.2	Type 3/Type 4
P3	15.8	Predominantly Type 3	11.8	Type 3	12.6	Type 3	-	-
			18.7	Type 2	18.1	Type 2		
P4	12.1	Predominantly Type 3	11.2	Type 3	12.0	Type 3	-	-
			18.2	Type 2	17.7	Type 2		

TABLE 2

MATERIAL PROPERTIES OF GRP TEST PANELS (Moduli and Strengths in $N/mm^2 \times 10^3$)

Panel No.	Shell Laminate						Frame Table						Frame Web					
	E_x	E_y	μ_{xy}*	G_{xy}*	Tensile Strength σ_{utx}	Compressive Strength σ_{ucx}	E_x*	E_y	μ_{xy}*	G_{xy}*	Tensile Strength σ_{uty}	Compressive Strength σ_{ucy}	E_x*	E_y	μ_{xy}*	G_{xy}*	Tensile Strength σ_{uty}	Compressive Strength σ_{ucy}
1	15.2	13.8	0.15	3.45	0.19	0.19	13.9	13.9	0.15	3.45	-	0.21	13.9	13.9	0.15	3.45	-	-
2	14.3	16.2	0.15	3.45	0.19	0.18	16.6	16.6	0.15	3.45	0.25	0.21	17.2	17.2	0.15	3.45	0.22	0.20
3	14.5	13.1	0.15	3.45	0.23	0.13	15.9	15.9	0.15	3.45	0.23	-	19.3	19.3	0.15	3.45	-	-
4	14.4	16.2	0.15	3.45	0.23	0.19	13.2	23.5	0.18	3.45	0.35	-	18.0	18.0	0.15	3.45	0.28	-
5	13.8	15.9	0.15	3.45	0.19	0.21	12.4	22.0	0.18	3.45	0.31	-	17.6	17.6	0.15	3.45	0.26	-
S2	14.7	16.2	0.15	3.45	0.22	0.20	16.7	16.7	0.15	3.45	0.27	0.21	16.8	16.8	0.15	3.45	0.28	0.18
S3	17.9	14.6	0.15	3.45	0.30	0.20	17.9	17.9	0.15	3.45	0.31	-	17.9	17.9*	0.15	3.45	-	-
S4	15.9	15.9*	0.15	3.45	0.21	0.15	17.0	23.0*	0.15	3.45	-	-	18.0	18.0*	0.15	3.45	-	-

*calculated value (no measurement made)

TABLE 1

GEOMETRY OF TEST PANELS (Dimensions in mm)

Panel No.	L	B	b_1	b_2	b_3	d	b_F	t_1 (= t_2)	t_3	t_4	Initial w_o(mm)	
											Inter-frame	Over-all
1	6096	1524	445	241	74	155	75	19.9	5.3	5.3	0.5	1.0
2	"	3048	673	330	292	305	114	31.8	29.0	16.5	0.2	1.5
3	"	1524	445	241	180	155	75	32.5	13.2	10.7	0.5	3.5
4	"	3048	508	236	216	235	89	38.4	35.3	15.4	0.8	2.5
5	"	3048	506	236	216	236	89	38.4	35.1	15.0	0.6	3.0
S2	1530	762	168	84	69	75	29	7.7	7.1	4.5	-	-
S3	"	380	112	60	42	38	24	6.1	2.5	2.5	-	-
S4	"	762	127	60	54	59	22	9.6	8.8	3.9	-	-
P1	1524	622	109	28	37	51	0	6.1	4.1	4.2	-	-
P2	"	533	108	29	36	51	0	6.2	3.6	3.5	-	-
P3	"	562	109	29	36	51	0	6.1	3.9	3.9	-	-
P4	"	579	109	29	36	51	0	6.1	3.9	3.7	-	-

REFERENCES

1. Smith C S: "Application of Fibre-Reinforced Plastics to Ship Structures" in "Developments in Thin-Walled Structures - Vol 2" (ed. Rhodes J and Walker A C), Applied Science Publishers, 1983.

2. Smith C S: "Buckling Problems in the Design of Fiberglass Reinforced Plastic Ships". J Ship Research, Vol 16, No 3, Sept 1972.

3. Smith C S: "Investigation of Ship Buckling Problems using Small-Scale Plastic Models". 5th Int Conf on Experimental Stress Analysis, Udine, May 1974.

4. Ball J: "Glass Reinforced Plastics for Marine Structures". Univ of Bath, School of Engineering, Report No 284, Feb 1974.

5. Adam T, Butler S: "The Static and Fatigue Strength of GRP Compression Structure". Univ of Bath, School of Engineering, Report No 355, Sept 1975.

6. Smith C S: "Structural Problems in the Design of GRP Ships". Proc of Sympos on GRP Ship Construction, RINA, London, Oct 1972.

7. Smith C S: "Elastic Analysis of Stiffened Plating under Lateral Loading". Trans RINA, Vol 108, 1966.

8. Smith C S: "Bending, Buckling and Vibration of Orthotropic Plate-Beam Structures" J Ship Research, Vol 12, No 4, Dec 1968.

9. Wittrick W H: "A Unified Approach to the Initial Buckling of Stiffened Panels in Compression". Aeronaut Quarterly, Vol XIX, p 265, 1968.

10. Wittrick W H, Williams F W: "Buckling and Vibration of Anisotropic or Isotropic Plate Assemblies under Combined Loadings". Int J Mech Sci, Vol 16, p 209, 1974.

11. Viswanathan A V, Tamekuni M, Baker L L: "Elastic Stability of Laminated Flat and Curved Long Rectangular Plates Subjected to Combined In-Plane Loads". NASA-CR-2330, 1973.

12. Smith C S: "Compressive Strength of Welded Steel Ship Grillages". Trans RINA, Vol 117, 1975.

13. ASAS-NL User Manual, Version 6, Aug 1982.

14. Dixon R H, Ramsay B W, Usher P J: "Design and Build of HMS WILTON". Proc of Sympos on GRP Ship Construction, RINA, London, 1972.

15. Harrhy J: "Structural Design of Single Skin Glass Reinforced Plastic Ships". Proc of Sympos on GRP Ship Construction, RINA, London, 1972.

16. Johnson A F: "Engineering Design Properties of GRP". British Plastics Fed, Publication No 215/1.

distributed, a reasonable permissible level of N_x for design purposes might be $N_{xp} = N_{xcr}\ (\bar{\beta} - 3.1\ \sigma)$, corresponding to a probability 0.999 that $N_{xu} > N_{xp}$: dotted lines representing these load-levels are shown in Figure 11. Because of the limited number and scope of experimental results, however, (influenced by geometric similarity of some of the test panels), values of σ_1 and σ_2 cannot be regarded as sufficiently accurate to provide a direct basis for design safety factors.

36. In previous ship designs (14,15) a factor of safety of 4 or more has been specified against calculated elastic buckling, reflecting uncertainty about the accuracy of calculations and the relationship of initial buckling stresses to structural collapse. Improved understanding of buckling failure combined with experience gained from ships in service indicates that this requirement is excessively conservative. As a compromise between past practice and the approximate statistical criteria discussed above, the following design approach is now suggested:-

(i) where the lowest initial buckling stress N_{xcr} is estimated accurately by folded-plate (or equivalent finite element) analysis, a permissible stress $N_{xp} = N_{xcr}/1.8$ should be adopted: this factor was chosen on an "engineering judgement" basis by applying a factor of 1/1.5 to a load-level at which significant damage might be expected to commence, judged from GRP panel tests to be about 15% below N_{xcr};

(ii) where N_{xcr} is estimated by use of the data curves in Figure 4, a supplementary factor of 1/1.2 should be applied to account for possible inaccuracy in the initial buckling stress, giving permissible $N_{xp} = N_{xcr}/2.25$.

Recommended permissible stresses, shown as full lines in Figure 11, evidently fall below mean collapse stresses (corresponding to $\bar{\beta}_1$ and $\bar{\beta}_2$) by 5.1 σ_1 and 5.5 σ_2 respectively.

37. It is assumed in the foregoing discussion that the dominant loading on a ship's hull is associated with wave action and is of short duration (5 to 10 seconds at most): recommended permissible stresses therefore make no allowance for creep. Where, exceptionally, design relates to a dead load it may be necessary to introduce an additional partial safety factor accounting for creep effects.

38. It should be noted finally that theoretical buckling stresses represented in Table 3 and Figure 11 and reflected in the above discussion of design requirements were based on mean, measured elastic moduli. For design purposes a supplementary partial safety factor accounting for variability of material properties should therefore be applied, or alternatively lower-bound material properties, obtained for example from Reference 16, should be adopted in design calculations.

ACKNOWLEDGEMENT

39. The author is indebted to colleagues at ARE, in particular Mr R S Dow and Mr W Kirkwood, for assistance in carrying out computation and experiments.

32. Results are summarized in Figure 14, which shows:

(a) compressive load-shortening curves for each type of buckling;

(b) curves of average compressive stress plotted against maximum lateral displacement;

(c) curves of maximum outer-fibre stress in the shell laminate for the lowest (Type-3) buckling stress, located at point D in Figure 13(a);

(d) distribution of longitudinal compressive stress across the shell laminate at various load levels.

It is evident that each type of buckling involves rapid growth of lateral deformation at compressive stresses approaching initial critical levels. Although, as in elastic columns, a stable post-buckling reserve of strength theoretically exists, such behaviour is pre-empted in panels of practical geometry by material failure, resulting from high bending stresses, before a significant increase in compressive load can develop beyond the initial critical level. Since initial distortions of moulded FRP structures are generally very small (those of Panels 4 and 5 were somewhat less than the smaller levels of w_o represented in Figure 14), large lateral displacements and hence outer-fibre material failure do not occur until compressive load closely approaches the lowest initial buckling stress: this critical stress therefore provides a good estimate of collapse strength.

DESIGN CONSIDERATIONS AND CONCLUSIONS

33. From the foregoing discussion it is evident that initial buckling stresses for longitudinally compressed, transversely stiffened FRP panels, as illustrated in Figure 2, may be estimated accurately by folded-plate analysis referring to local interframe instability. Care should be taken when carrying out such analysis to examine each of the interframe modes shown in Figure 3. A reasonable though somewhat less accurate estimate of initial buckling stress may be obtained from the data curves shown in Figure 4. Nonlinear finite element analysis has confirmed experimental observations in demonstrating that for FRP panels with typical, small imperfections, initial buckling stresses obtained by linear analysis provide a close approximation to collapse strength.

34. For practical design purposes it is suggested that preliminary estimates of initial buckling stress should be made using the data curves: at a later stage in design these should be checked using folded-plate analysis. Where folded-plate analysis is not available, linear finite element analysis, although less accurate and much more expensive, may be used instead to estimate initial buckling stresses. Where a structure is highly non-uniform or where unusual boundary conditions exist, finite element analysis may be the only way to obtain accurate results.

35. Specification of design safety factors against buckling failure should ideally be based on statistical correlation of theoretical buckling stresses and experimental collapse data. Ultimate compressive strengths N_{xu} may be related to theoretical initial buckling loads N_{xcr} by an empirically determined factor $\beta = N_{xu}/N_{xcr}$. From the theoretical and experimental results summarized in Table 3 and Figure 11, mean values of β referring to data curves and folded-plate analysis were found to be respectively $\bar{\beta}_1 = 1.079$ and $\bar{\beta}_2 = 1.070$, with standard deviations $\sigma_1 = 0.125$ and $\sigma_2 = 0.093$. Assuming that β is normally

that integrals $\int_0^L w_i\, w_j\, dx$ ($i \neq j$) were usually less than 1% and in almost all cases less than 10% of integrals $\int_0^L w_j^2\, dx$.

28. Assuming in accordance with linear theory that modal displacements become infinitely large at critical stress levels, an experimentally-based estimate of buckling load for each theoretical mode may be found by extrapolation from a plot of σ_x/a_{jk} against the experimental compressive stress σ_x, as illustrated in Figure 12 for Panel 5. Theoretical Modes 1 to 4, shown in Figure 9, were used in this case to define w_j. From Figure 12 it is clear that Mode 2 deformations are dominant over most of the pre-collapse load range, giving an extrapolated buckling stress which is consistent with the theoretical value of 72.8 N/mm^2. Mode 4 deformations are also present and the extrapolated buckling stress is close to the theoretical value of 90.3 N/mm^2. Mode 1 deformations are not evident during the early stages of load application but emerge strongly just before collapse. No meaningful Mode 3 deformation components were identified.

29. The procedure outlined above, which is a variant of the Southwell plot technique, has also been used successfully in the interpretation of buckling experiments on small-scale perspex models (3).

Nonlinear Buckling Analysis

30. In order to obtain an improved understanding of the failure process including information on postbuckling behaviour and imperfection sensitivity, nonlinear analysis of interframe buckling in Panel 5 has been carried out using the general purpose finite element program ASAS-NL (13), implemented on the VAX 11/780 computer at ARE. Three different finite element models were examined, as shown in Figure 13, in order to represent Type-3, Type-2 and Type-1 buckling. Eight-node isoparametric quadrilateral shell elements were used throughout. Large displacements were handled using an updated Langrangian (moving co-ordinate) formulation with application of a modified Newton-Raphson iterative equilibrium correction. Anisotropic material properties, as defined in Table 2, were assumed to remain constant at all load-levels.

31. Referring to Figure 13, boundary conditions were assumed as follows:

(i) plane of symmetry at AB ($u = \partial v/\partial x = \partial w/\partial x = 0$);

(ii) "moving" plane of symmetry at CD ($\partial v/\partial x = \partial w/\partial x = 0$);

(iii) longitudinal plane of symmetry at the panel centreplane BD ($v = \partial u/\partial y = \partial w/\partial y = 0$);

(iv) simple support at the panel edge AC ($w = 0$, otherwise unconstrained).

Compressive load was applied incrementally by imposing uniform end-shortening displacements δ on the plane CD. Initial deformations of the shell laminate were assumed to have approximately the same form as the appropriate interframe buckling mode with sinusoidal distribution in x and y-directions and an amplitude w_o: in each case two distortion amplitudes, $w_o/B = 0.0002$, 0.001, were considered.

DEFINITION OF PANEL DIMENSIONS

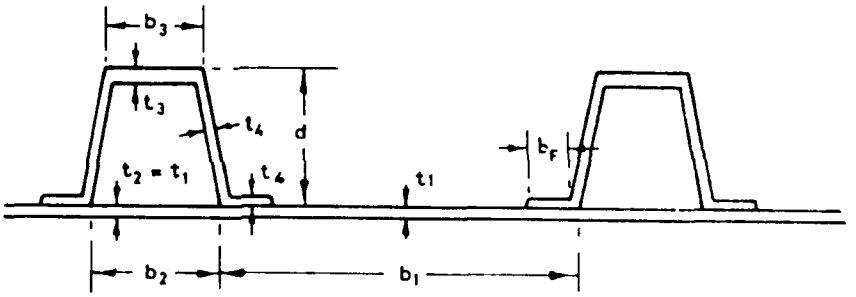

FIGURE 6

COMPRESSION TEST RIG (PANEL 2)

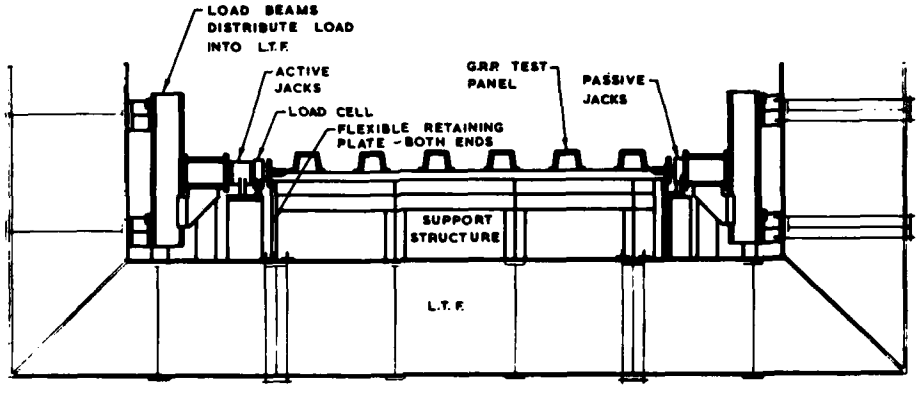

SL72/116/18

FIGURE 7

PANEL 5 FOLLOWING COLLAPSE

FIGURE 8

PANEL 5: EXPERIMENTAL DEFORMATIONS AND THEORETICAL BUCKLING MODES

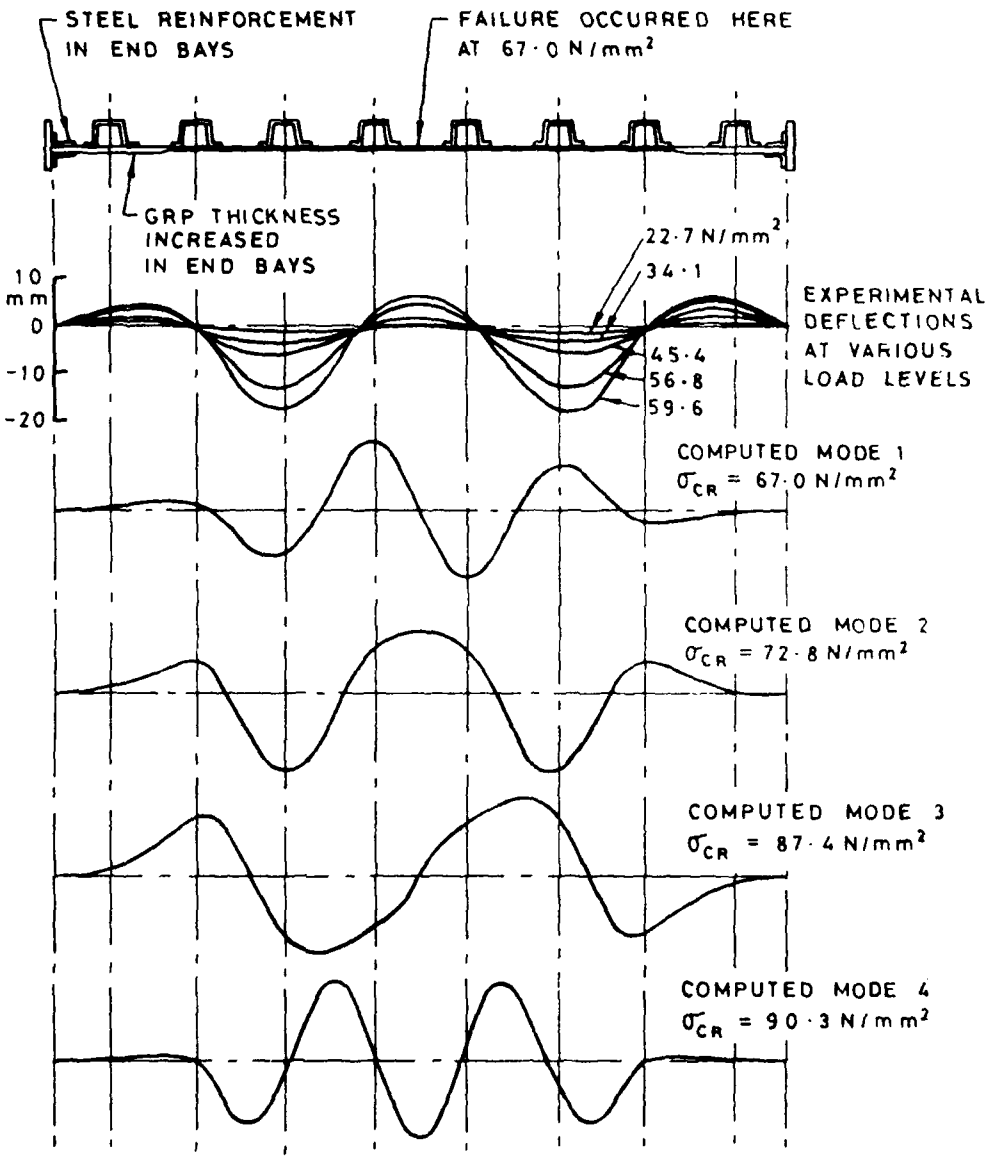

FIGURE 9

PANEL 4: EXPERIMENTAL DEFORMATIONS

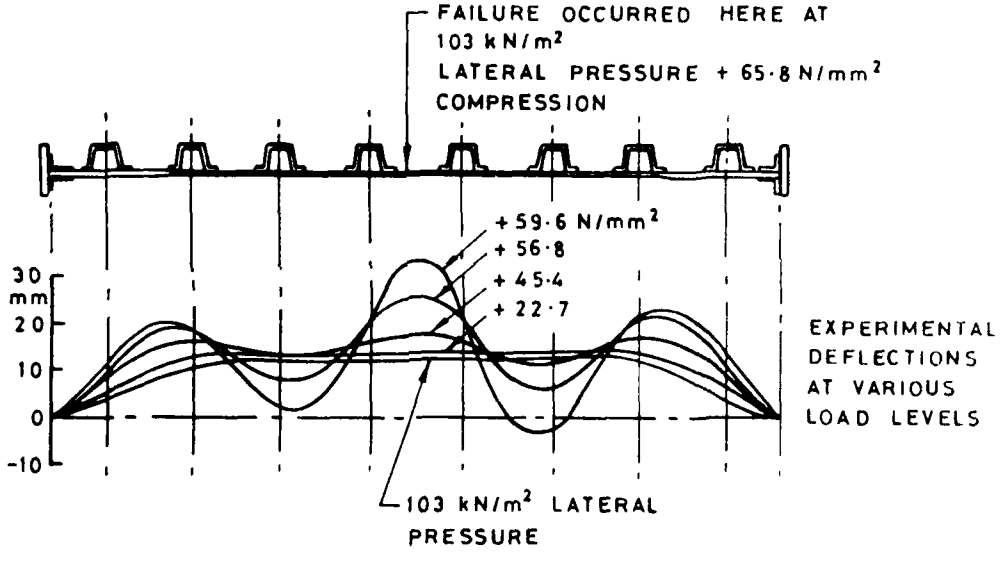

FIGURE 10

CORRELATION OF THEORETICAL BUCKLING STRESSES AND EXPERIMENTAL COLLAPSE STRENGTHS

EXPERIMENTAL DATA
- × LARGE - SCALE GRP PANELS
- ⊙ SMALL - SCALE GRP PANELS
- △ SMALL - SCALE PERSPEX PANELS

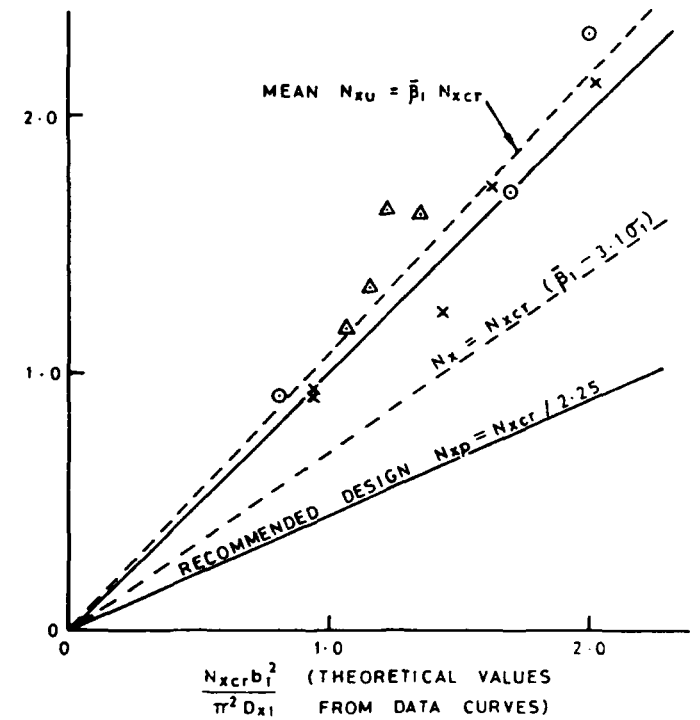

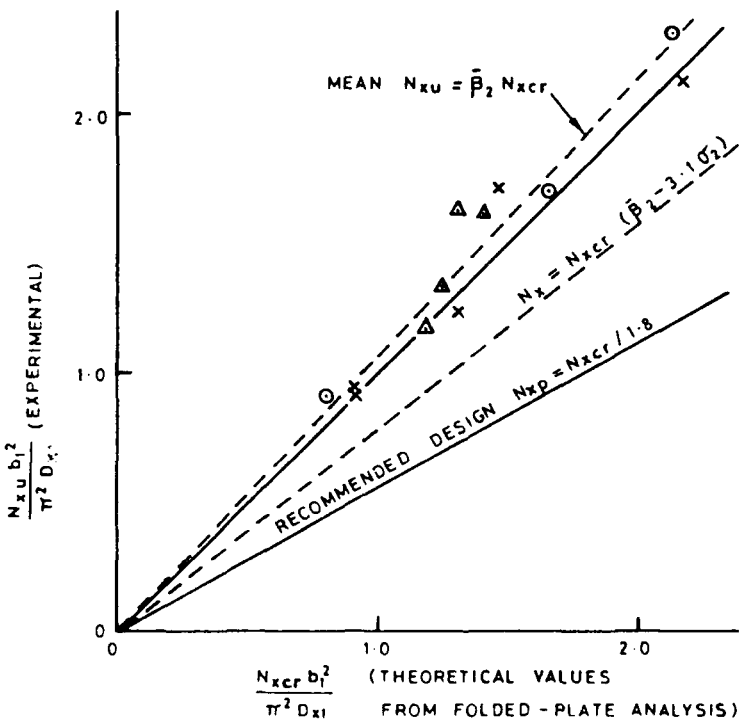

FIGURE 11

MODAL PLOTS FOR PANEL 5

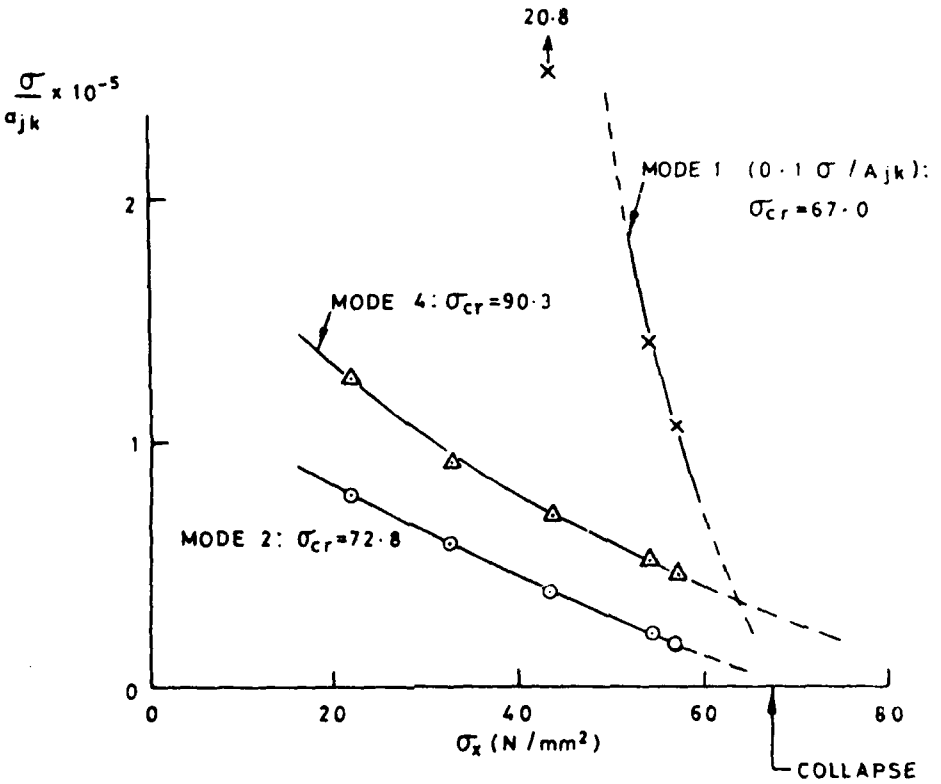

FIGURE 12

FINITE ELEMENT MODELS FOR NONLINEAR BUCKLING ANALYSIS

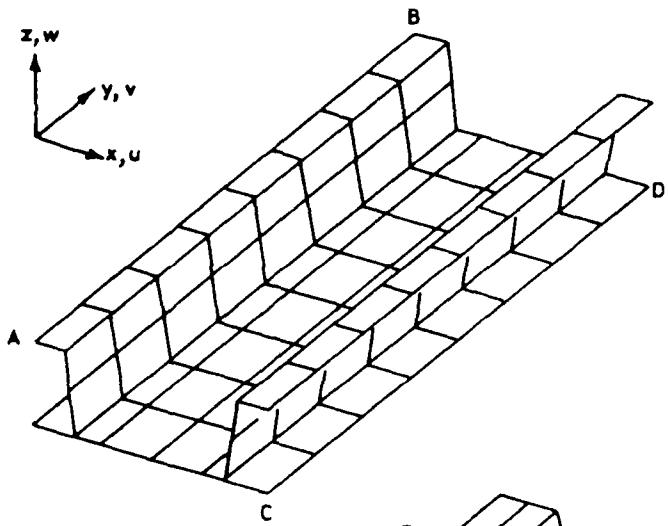

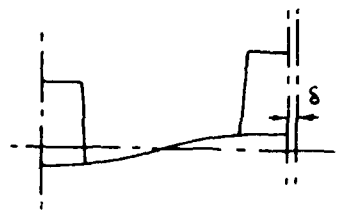

TYPE 3 BUCKLING

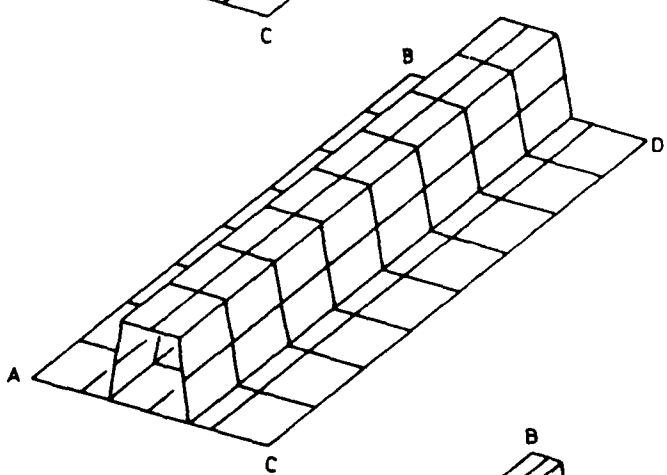

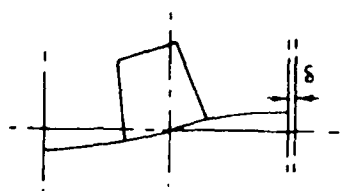

TYPE 2 BUCKLING

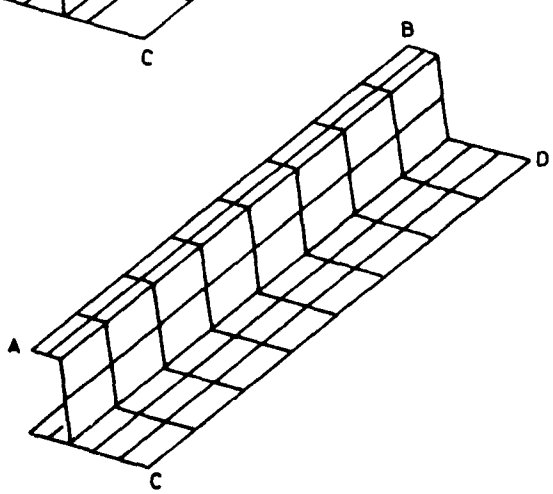

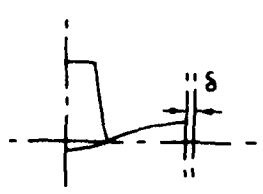

TYPE 1 BUCKLING

FIGURE 13

RESULTS OF NONLINEAR FINITE ELEMENT ANALYSIS

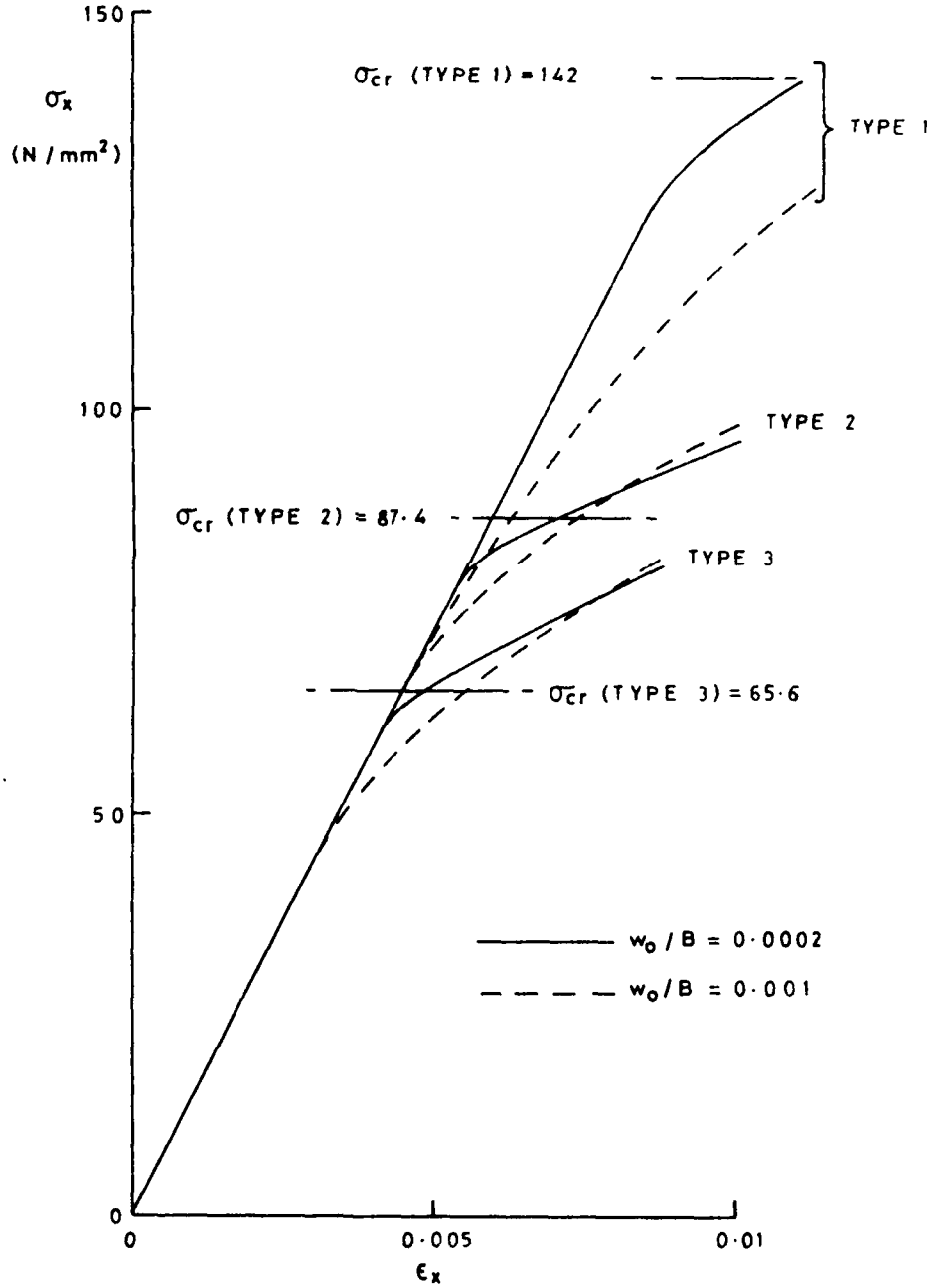

(a) LOAD - SHORTENING CURVES

FIGURE 14

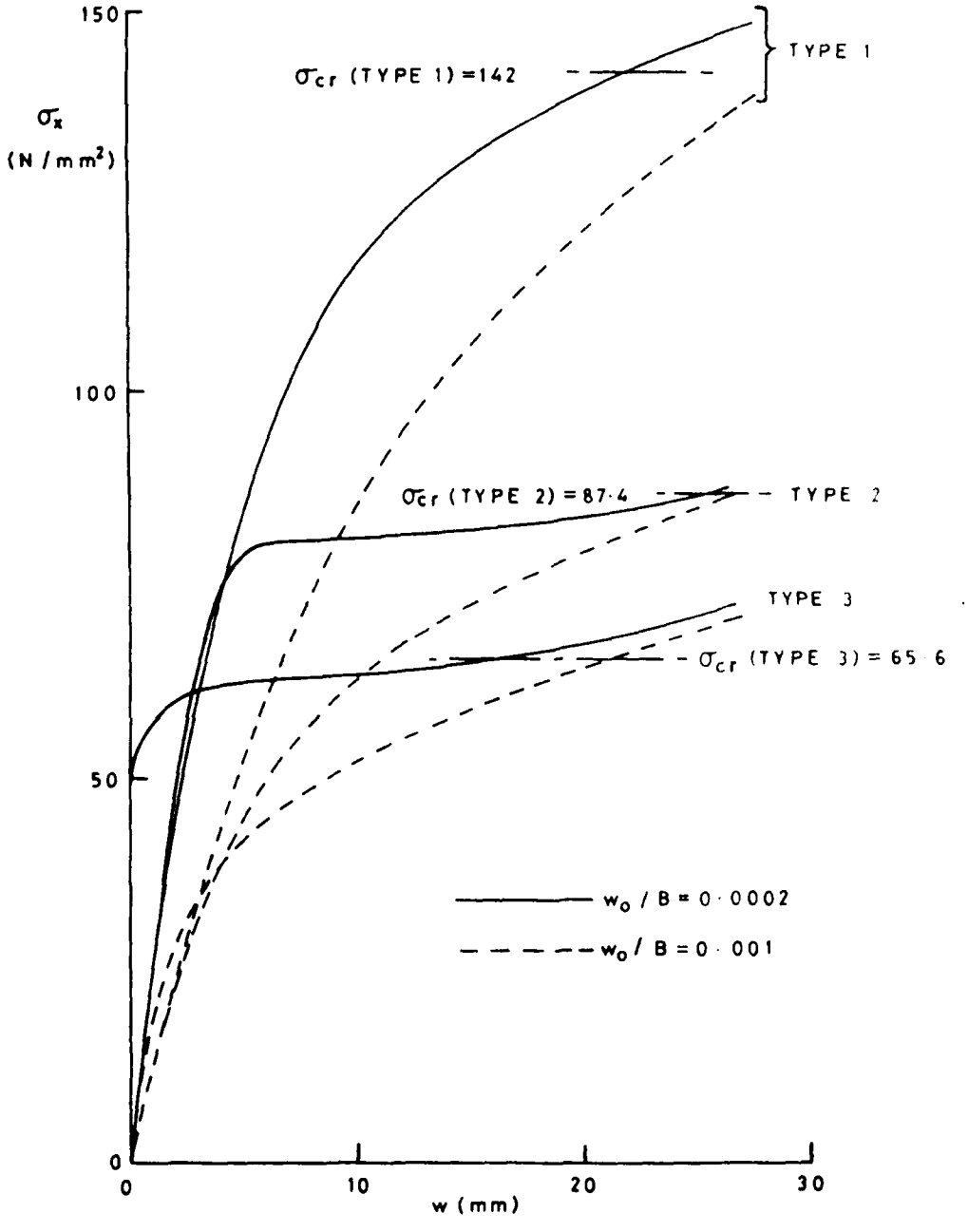

(b) LOAD / LATERAL DISPLACEMENT

FIGURE 14 (contd)

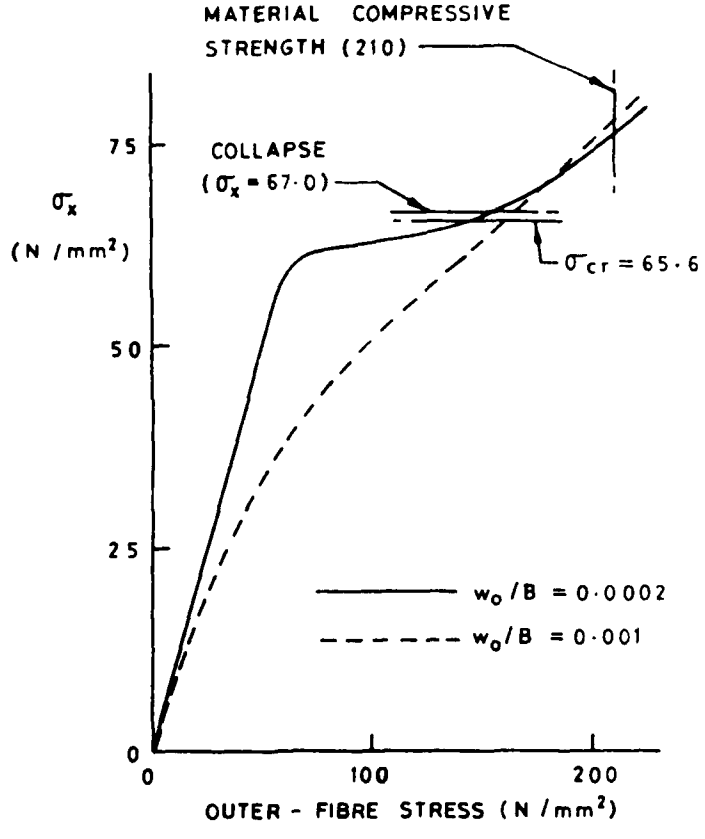

(c) MAXIMUM LAMINATE STRESS

FIGURE 14 (contd)

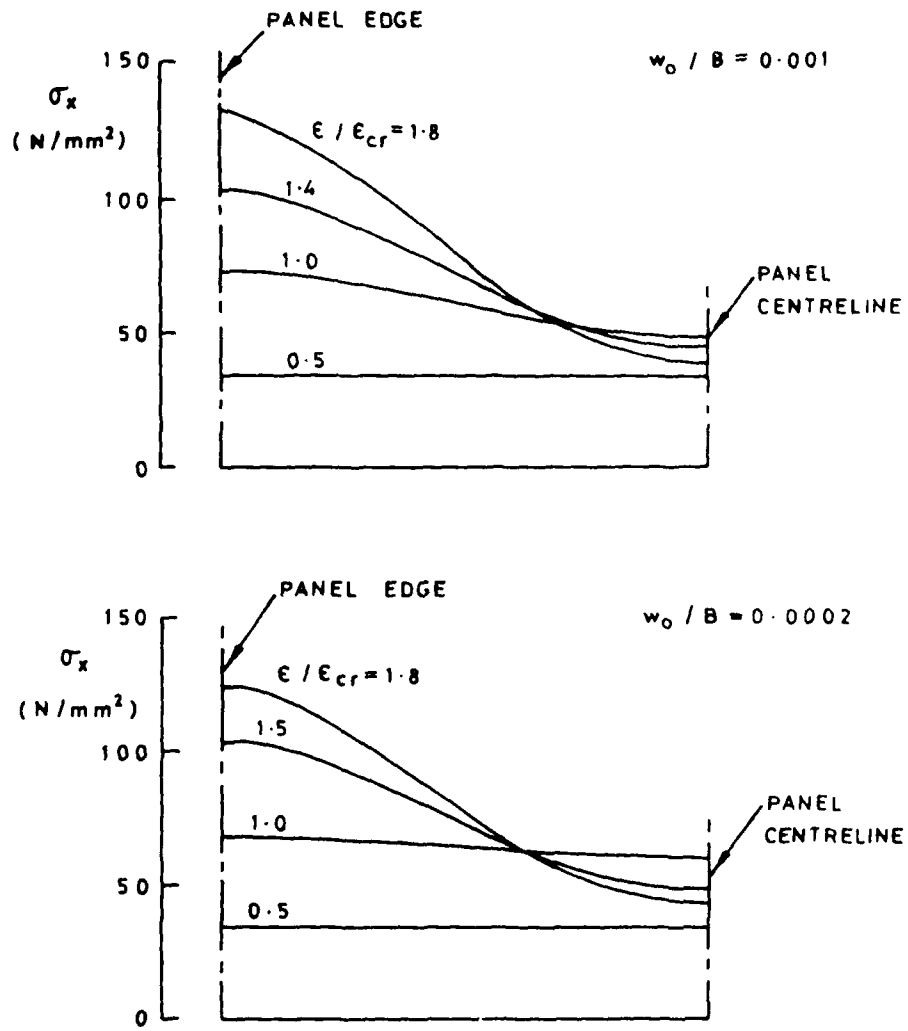

(d) DISTRIBUTION OF COMPRESSIVE STRESS ACROSS PANEL
(TYPE 3 BUCKLING $\epsilon_{cr} = \sigma_{cr} / E_x$)

FIGURE 14 (contd)

DOCUMENT CONTROL SHEET

(Notes on completion overleaf)

Overall security classification of sheet ..... UNLIMITED .....

(As far as possible this sheet should contain only unclassified information. If it is necessary to enter classified information, the box concerned must be marked to indicate the classification eg (R), (C) or (S)).

1. DRIC Reference (if known)	2. Originator's Reference	3. Agency Reference	4. Report Security Classification
	AMTE(S)/R84104		UNLIMITED

5. Originator's Code (if known)	6. Originator (Corporate Author) Name and Location
	Admiralty Research Establishment Dunfermline St Leonard's Hill, Dunfermline, Fife, KY11 5PW
5a. Sponsoring Agency's Code (if known)	6a. Sponsoring Agency (Contract Authority) Name and Location

7. Title

DESIGN OF TRANSVERSELY STIFFENED FRP PANELS UNDER COMPRESSIVE LOAD

7a. Title in Foreign Language (in the case of translations)

7b. Presented at (for conference papers). Title, place and date of conference

8. Author 1,Surname,initials	9a. Author 2	9b. Authors 3, 4...	10. Date	pp	ref
SMITH, C S			12.1984	42	16

11. Contract Number	12. Period	13. Project	14. Other References

15. Distribution statement

Distribution controlled by MOD Technical Policy Authority, Research Area Leader 1, CS, ARE Dunfermline.

Descriptors (or keywords)

GRP
Stiffened Panels
Compressive Buckling
Postbuckling
Finite element analysis
Test results
Design

Summary

A review is made of the problem of buckling failure in fibre-reinforced plastic panels having stiffeners of chat section under compressive load acting across the line of the stiffeners. This problem is of practical importance in the design of FRP ships. Alternative analysis methods are discussed, including use of approximate data curves and folded-plate analysis to determine initial buckling behaviour, together with nonlinear finite element analysis referring to imperfection effects and post-buckling behaviour. Some previously unreported experimental results are described. These, together with previously published test data, are correlated with theoretical analysis as a basis for making updated design recommendations. Originator Supplied Keywords include:

AMTE(S)/R84104 UNLIMITED
DESIGN OF TRANSVERSELY STIFFENED FRP PANELS UNDER COMPRESSIVE LOAD by C S Smith, 1984

A review is made of the problem of buckling failure in fibre-reinforced plastic panels having stiffeners of "hat" section under compressive load acting across the line of the stiffeners. This problem is of practical importance in the design of FRP ships. Alternative analysis methods are discussed, including use of approximate data curves and folded-plate analysis to determine initial buckling behaviour, together with nonlinear finite element

SUBJECT INDEX

GRP
Stiffened Panels
Compressive Buckling
Postbuckling
Finite element analysis
Test results
Design

AMTE(S)/R84104 UNLIMITED
DESIGN OF TRANSVERSELY STIFFENED FRP PANELS UNDER COMPRESSIVE LOAD by C S Smith, 1984

A review is made of the problem of buckling failure in fibre-reinforced plastic panels having stiffeners of "hat" section under compressive load acting across the line of the stiffeners. This problem is of practical importance in the design of FRP ships. Alternative analysis methods are discussed, including use of approximate data curves and folded-plate analysis to determine initial buckling behaviour, together with nonlinear finite element

SUBJECT INDEX

GRP
Stiffened Panels
Compressive Buckling
Postbuckling
Finite element analysis
Test results
Design

AMTE(S)/R84104 UNLIMITED
DESIGN OF TRANSVERSELY STIFFENED FRP PANELS UNDER COMPRESSIVE LOAD by C S Smith, 1984

A review is made of the problem of buckling failure in fibre-reinforced plastic panels having stiffeners of "hat" section under compressive load acting across the line of the stiffeners. This problem is of practical importance in the design of FRP ships. Alternative analysis methods are discussed, including use of approximate data curves and folded-plate analysis to determine initial buckling behaviour, together with nonlinear finite element

SUBJECT INDEX

GRP
Stiffened Panels
Compressive Buckling
Postbuckling
Finite element analysis
Test results
Design

AMTE(S)/R84104 UNLIMITED
DESIGN OF TRANSVERSELY STIFFENED FRP PANELS UNDER COMPRESSIVE LOAD by C S Smith, 1984

A review is made of the problem of buckling failure in fibre-reinforced plastic panels having stiffeners of "hat" section under compressive load acting across the line of the stiffeners. This problem is of practical importance in the design of FRP ships. Alternative analysis methods are discussed, including use of approximate data curves and folded-plate analysis to determine initial buckling behaviour, together with nonlinear finite element

SUBJECT INDEX

GRP
Stiffened Panels
Compressive Buckling
Postbuckling
Finite element analysis
Test results
Design

analysis referring to imperfection effects and post-buckling behaviour. Some previously unreported experimental results are described. These, together with previously published test data, are correlated with theoretical analysis as a basis for making updated design recommendations.	analysis referring to imperfection effects and post-buckling behaviour. Some previously unreported experimental results are described. These, together with previously published test data, are correlated with theoretical analysis as a basis for making updated design recommendations.
analysis referring to imperfection effects and post-buckling behaviour. Some previously unreported experimental results are described. These, together with previously published test data, are correlated with theoretical analysis as a basis for making updated design recommendations.	analysis referring to imperfection effects and post-buckling behaviour. Some previously unreported experimental results are described. These, together with previously published test data, are correlated with theoretical analysis as a basis for making updated design recommendations.


DAT
FILM